Towards 21-cm Intensity Mapping with uGMRT

Khandakar Md Asif Elahi, IIT Kharagpur, India.

with Somnath Bharadwaj, Abhik Ghosh, Srijita Pal, Sk. Saiyad Ali, Samir Choudhuri, Arnab Chakraborty, Abhirup Datta, Nirupam Roy, Madhurima Choudhury and Prasun Dutta.

MNRAS: https://doi.org/10.1093/mnras/stad191
ARXIV: https://arxiv.org/abs/2301.06677v1

The 21 cm Line

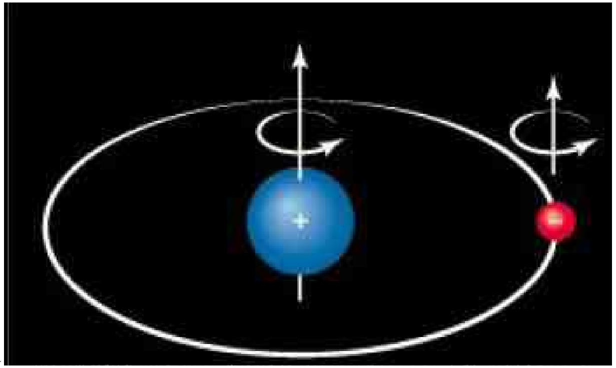

1s

$\Delta E = 6\ \mu eV$

$\nu = 1420\ MHz$

$\lambda = 21\ cm$

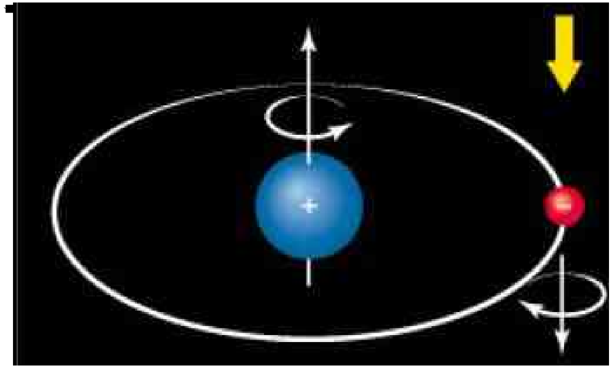

ground state of neutral Hydrogen has two Hyperfine levels

Cosmology with the 21 cm line

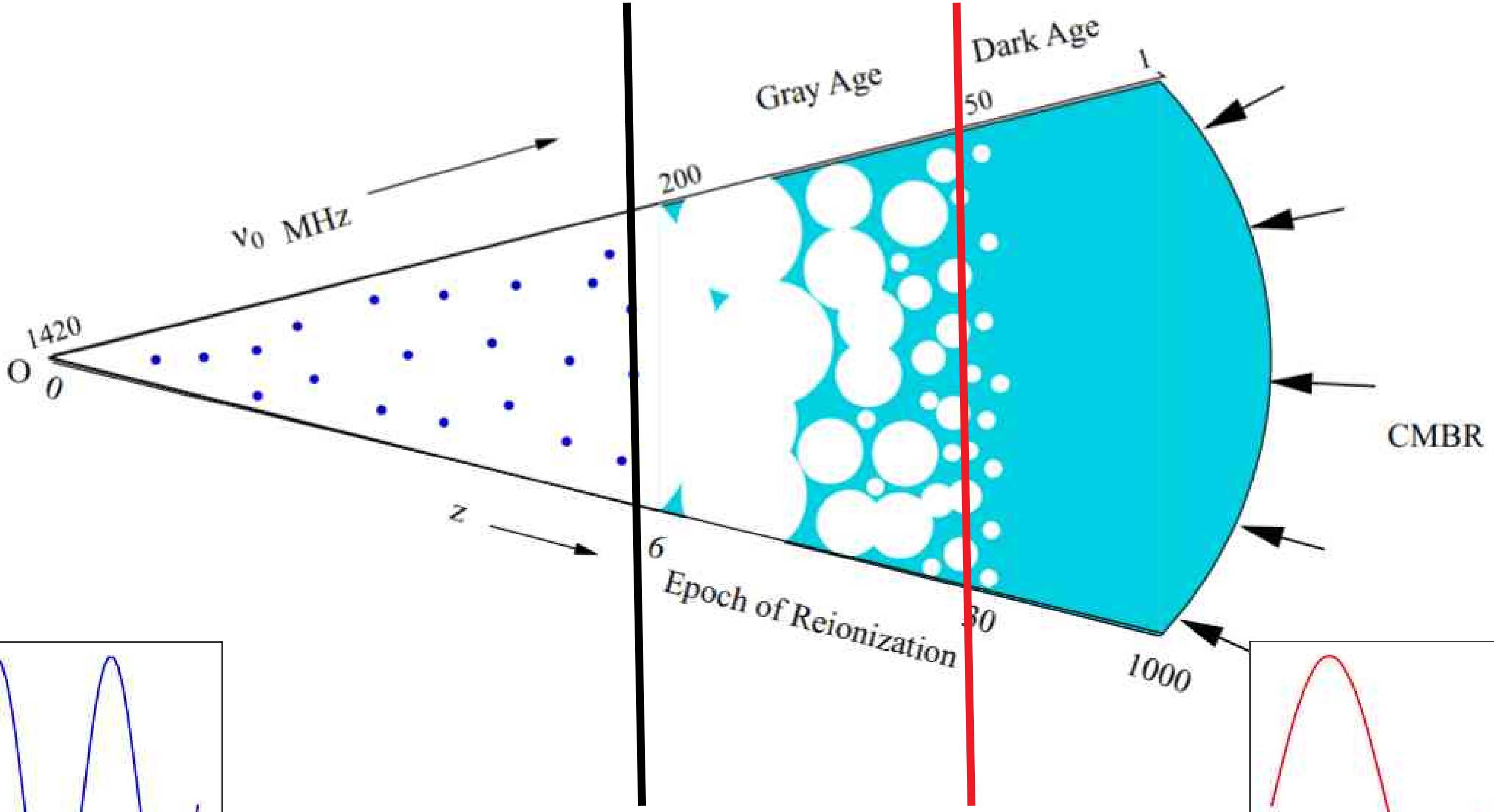

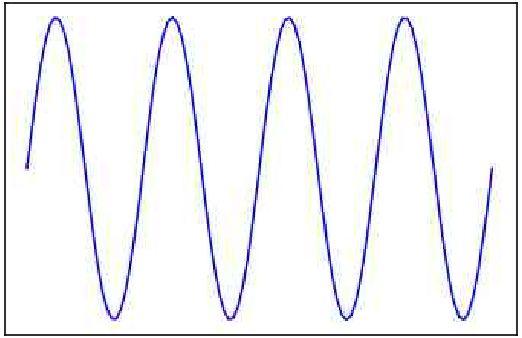

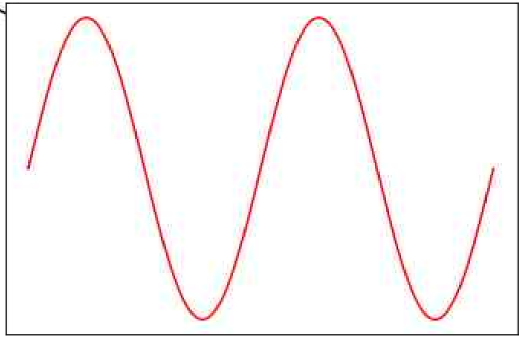

$$1+z = 1420/\nu$$

Cosmology with 21 cm line

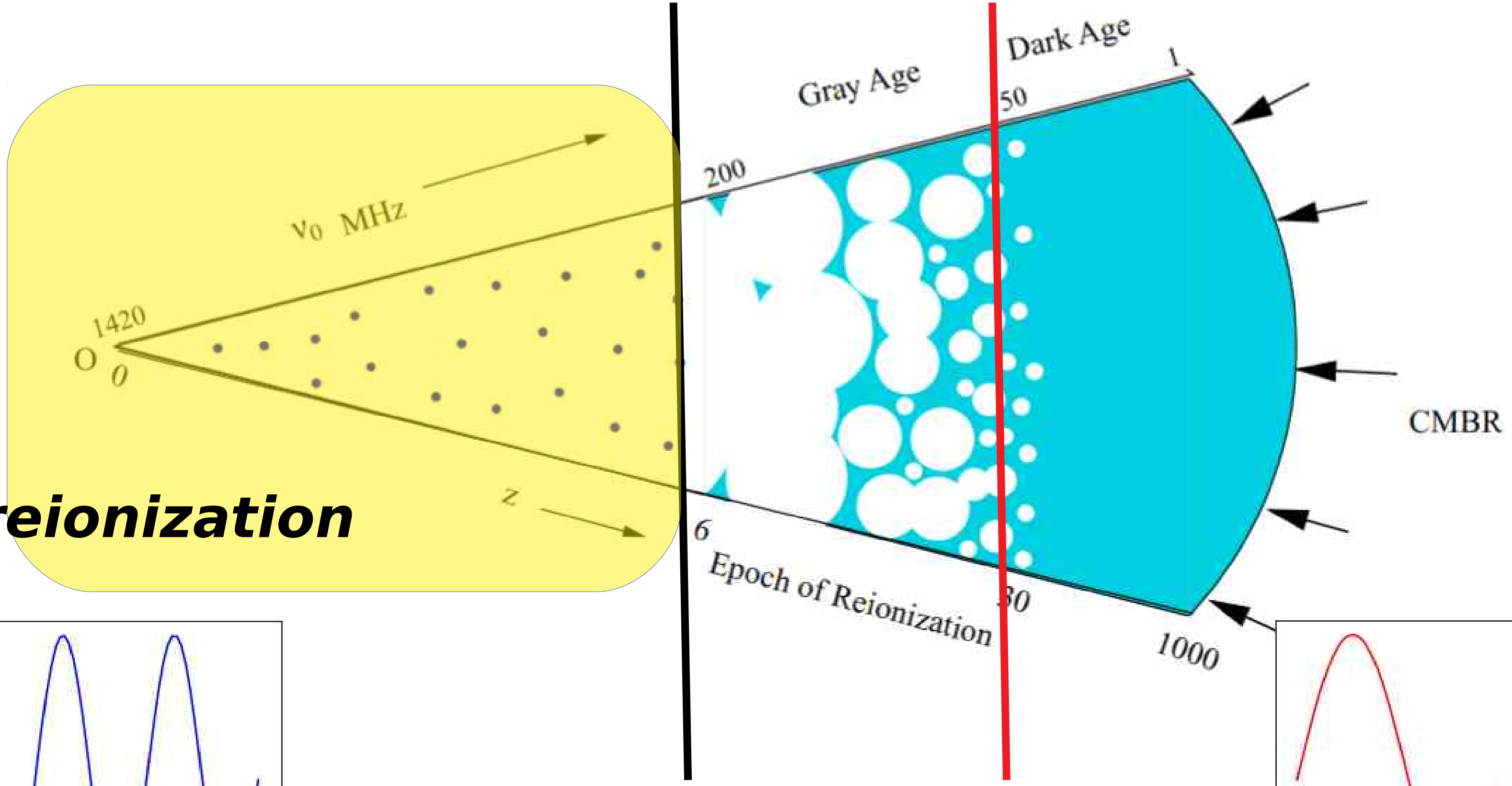

post-reionization

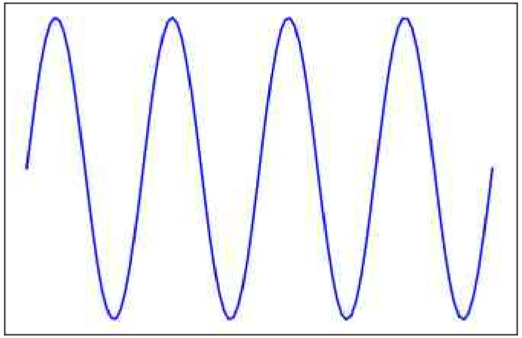

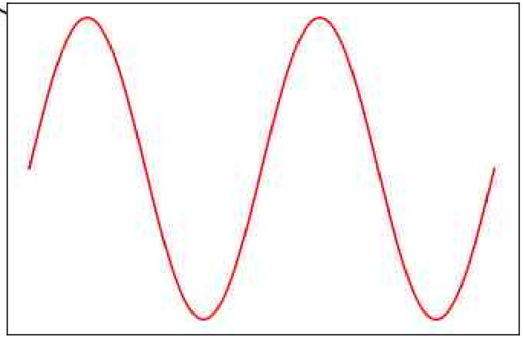

$1+z = 1420/\nu$

21 cm Intensity Mapping (IM)

Single Dish
e.g. GBT

Interferometry

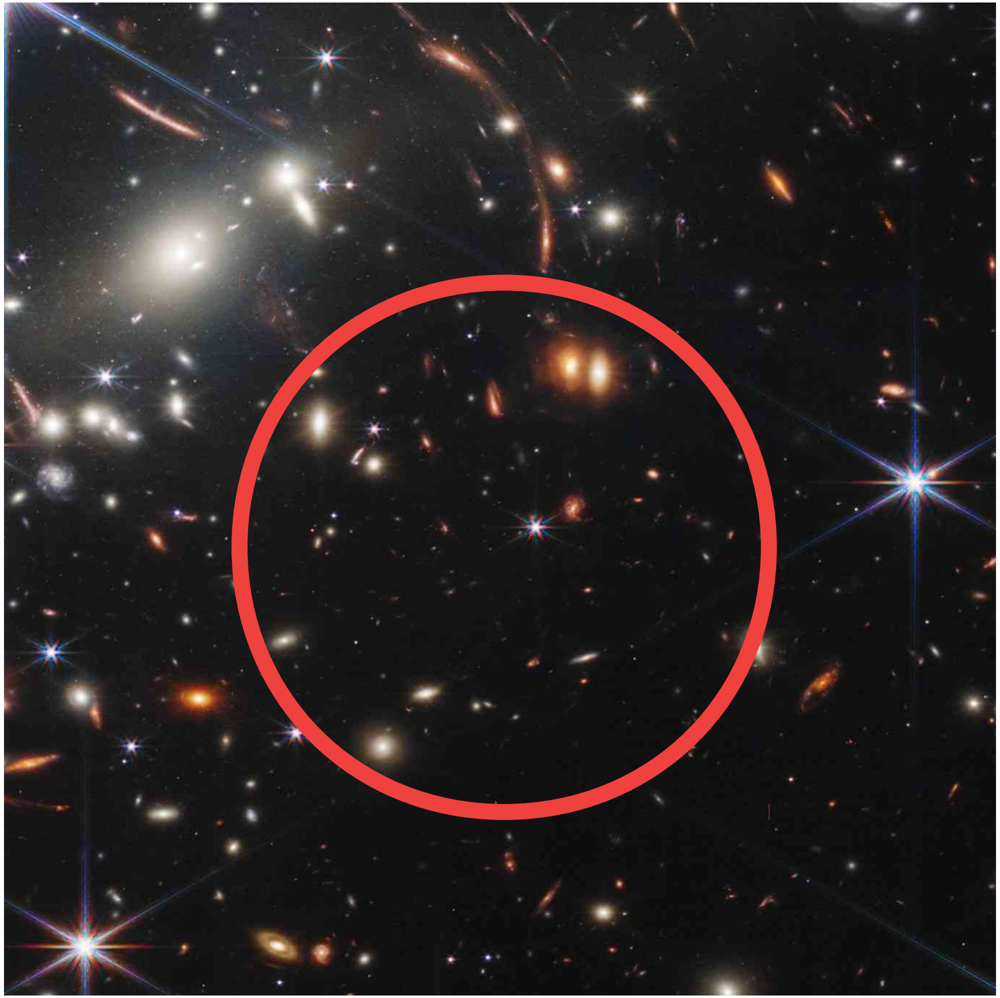

21 cm IM Experiments

21 cm IM Experiments

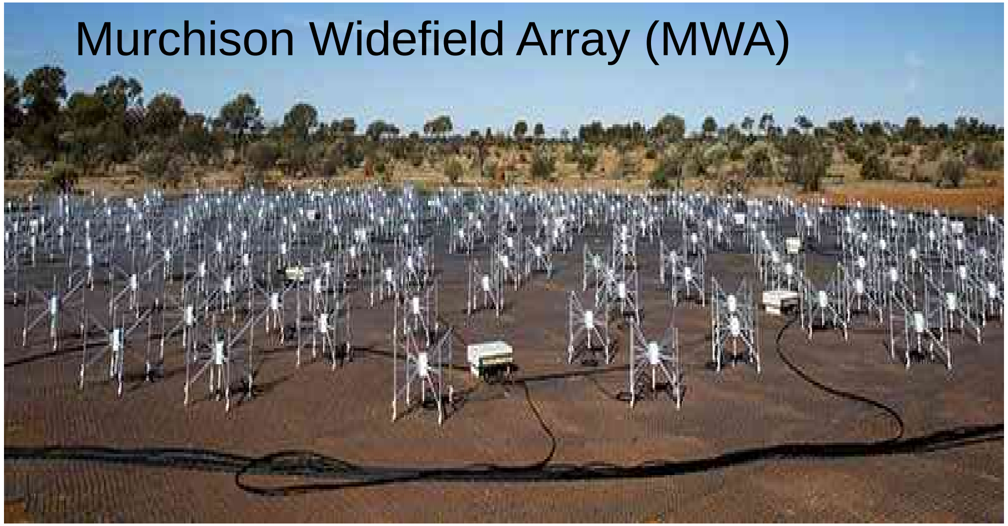

Data

Table 1. Observation summary.

Working antennas	28
Central frequency	400 MHz
Number of channels	8192
Channel width	24.4 kHz
Bandwidth	200 MHz
Total observation time	25 h
Integration time	2 s
Target field $(\alpha, \delta)_{2000}$	$(16^h 10^m 1^s, +54^\circ 30' 36'')$
Galactic coordinates (l, b)	$86.95^\circ, +44.48^\circ$

Flagging, calibration, imaging

Chakraborty et al., 2019
10.1093/mnras/stz2533
arXiv:1908.10380

Data used here

Bandwidth	24.4 MHz
ν_c	432.8 MHz
$\Delta\nu$	24.4 kHz

Pal, **Elahi**, Bharadwaj + others, 2022
10.1093/mnras/stac2419
arXiv:2208.11063

Elahi, Bharadwaj + others 2023
10.1093/mnras/stad191
arXiv:2301.06677

21 cm IM Statistics

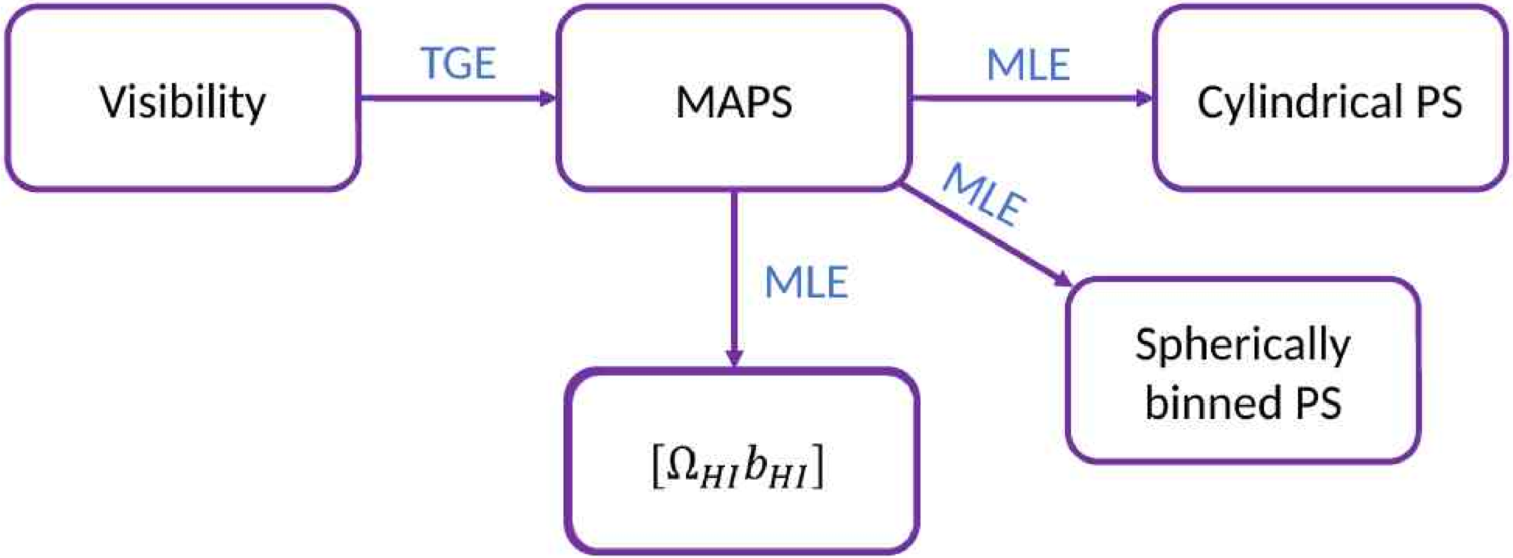

21 cm IM Statistics

Visibility

$$\mathcal{V}(\boldsymbol{U},\nu) = \left(\frac{\partial B}{\partial T_b}\right) \int d^2\theta \mathcal{A}(\theta,\nu)\delta T_b(\theta,\nu) e^{-2\pi i \boldsymbol{U}\cdot\theta}$$

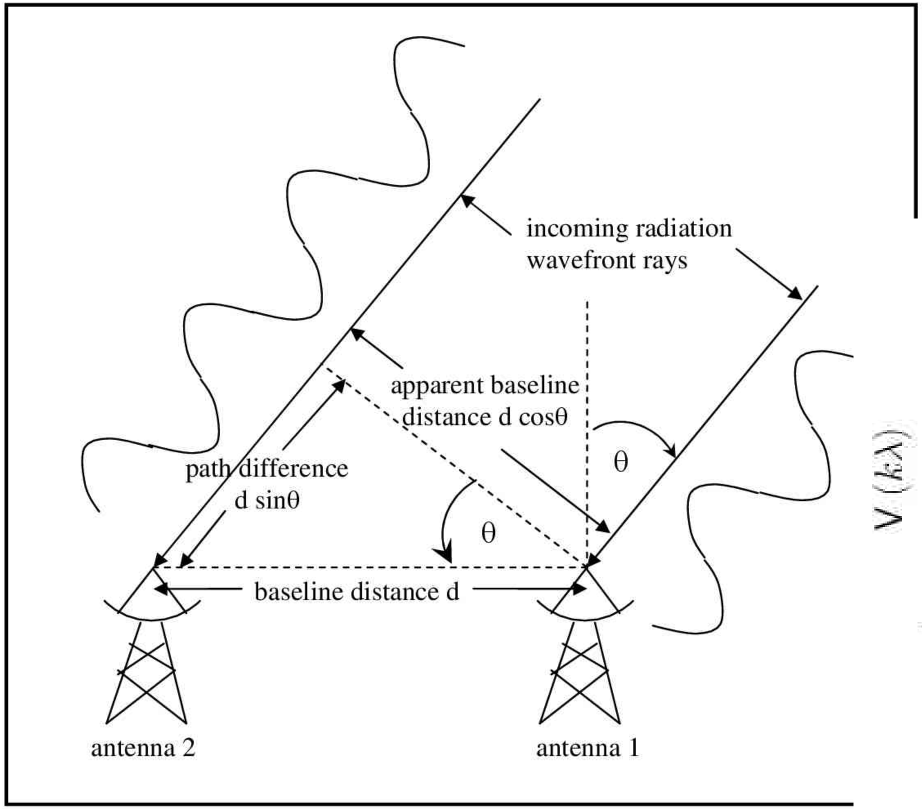

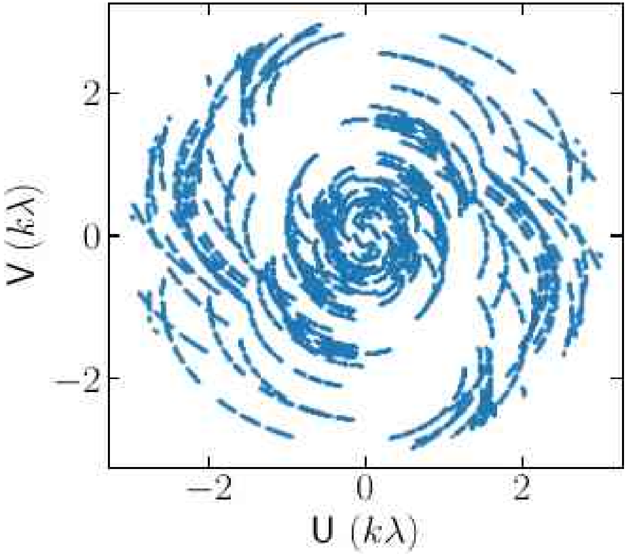

21 cm IM Statistics

Multifrequency Angular Power Spectrum

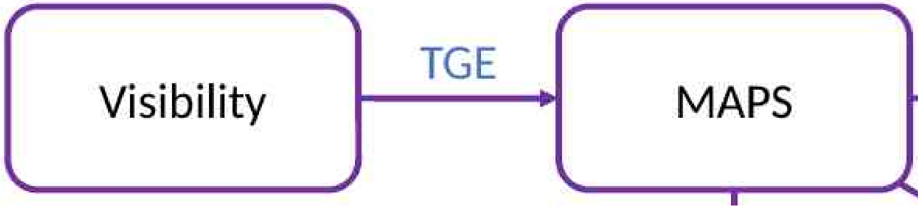

$$\delta T_b(\hat{\mathbf{n}}, \nu) = \sum_{\ell,m} a_{\ell m}(\nu) Y_\ell^m(\hat{\mathbf{n}})$$

$$C_\ell(\nu_a, \nu_b) = \langle a_{\ell m}(\nu_a) a^*_{\ell m}(\nu_b) \rangle$$

$$C_\ell(\nu_a, \nu_b) = C_\ell(|\nu_a - \nu_b|) = C_\ell(\Delta\nu) \ \ (\text{ergodic})$$

Oscillations? Foregrounds

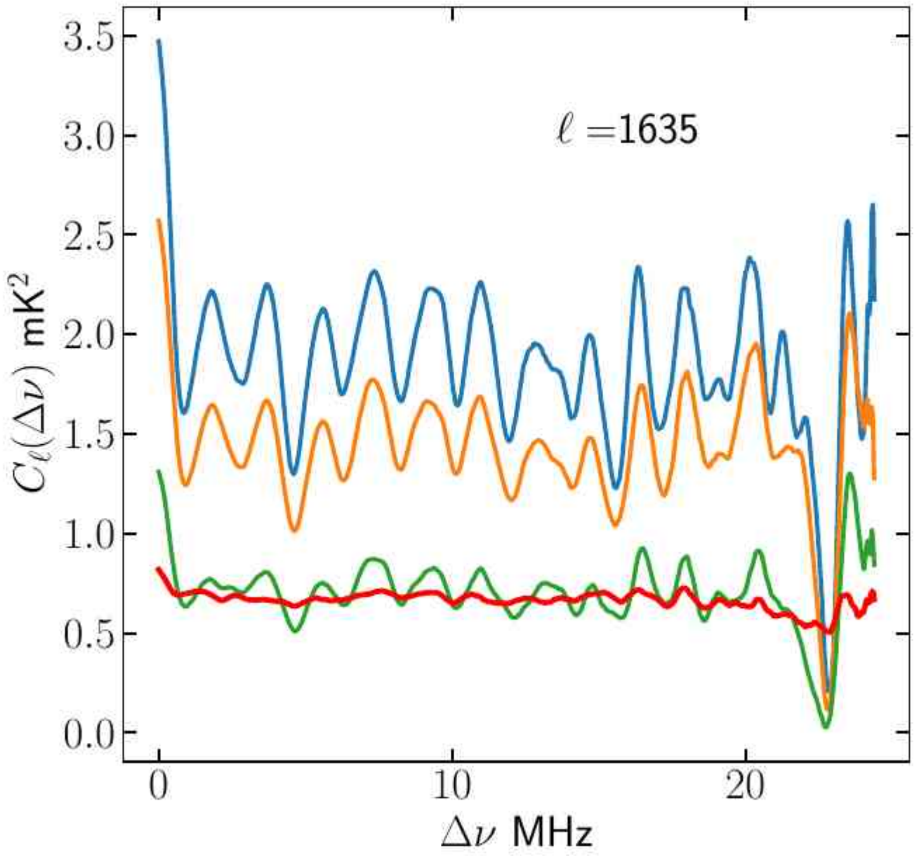

Tapered Gridded Estimator (TGE)

$$\mathcal{V}_{cg}^{X}(\nu) = \sum_{i} \tilde{w}(\mathbf{U}_g - \mathbf{U}_i)\,\mathcal{V}_i^{X}(\nu)\,F_i^{X}(\nu)$$

(Cross) TGE

$$\mathcal{W}(\theta) = e^{-\theta^2/f^2\theta_0^2}$$

$$\hat{E}_g = M_g^{-1} \mathcal{R}e\left[\mathcal{V}_{cg}^{RR} \otimes \mathcal{V}_{cg}^{*LL} + \mathcal{V}_{cg}^{LL} \otimes \mathcal{V}_{cg}^{*RR}\right]$$

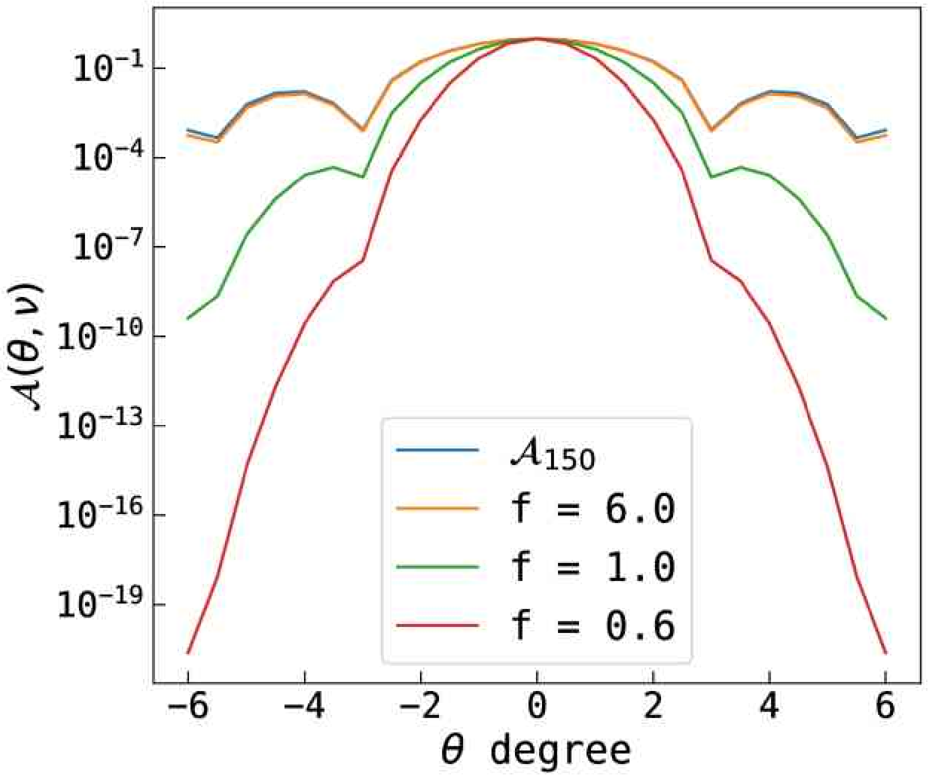

Foreground mitigation by tapering

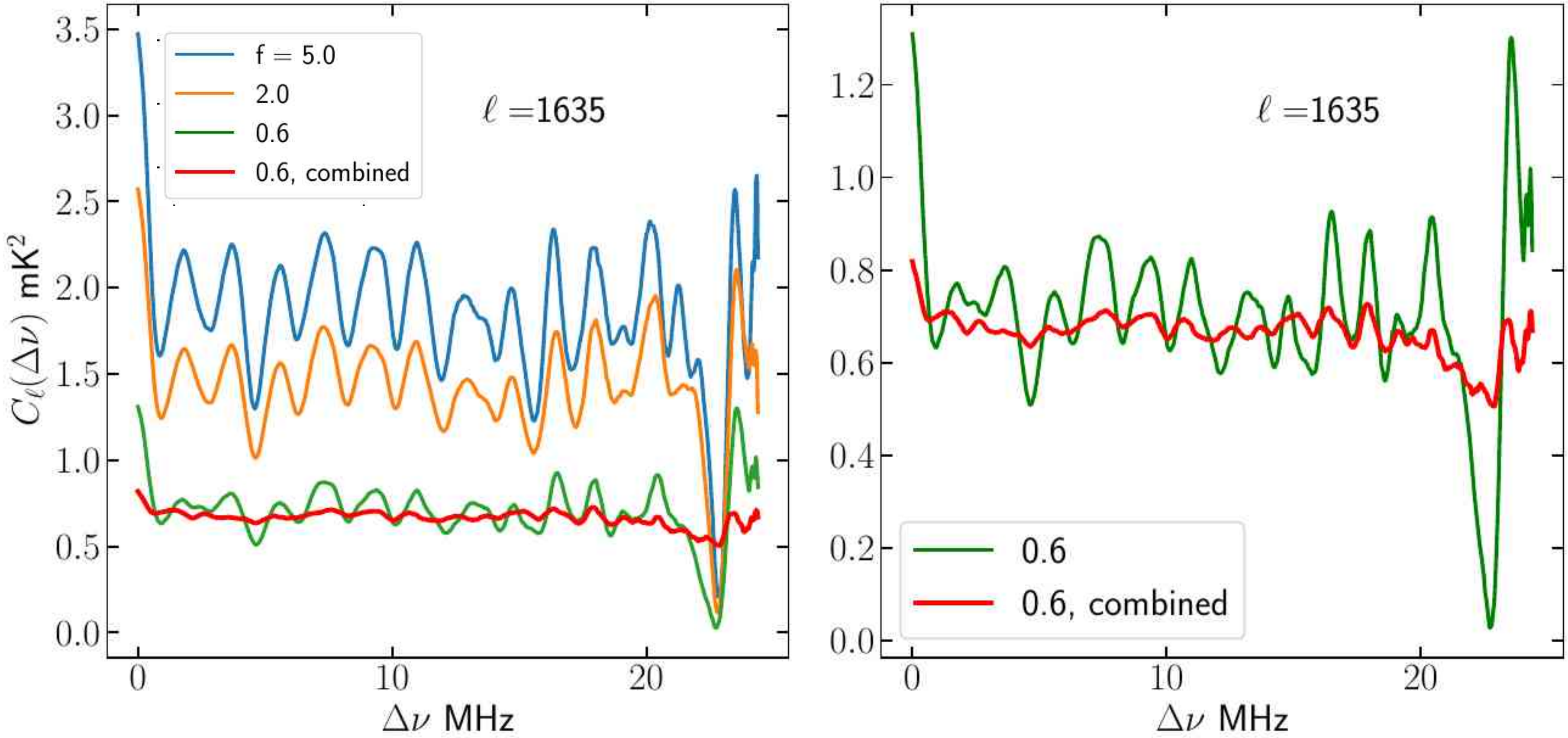

(Total) TGE
Paper I (Pal et al. 2022)

Cross TGE

$$P(\mathbf{k}_\perp, k_\parallel) = r^2 r' \int_{-\infty}^{\infty} d(\Delta\nu) e^{-ik_\parallel r' \Delta\nu} C_\ell(\Delta\nu)$$

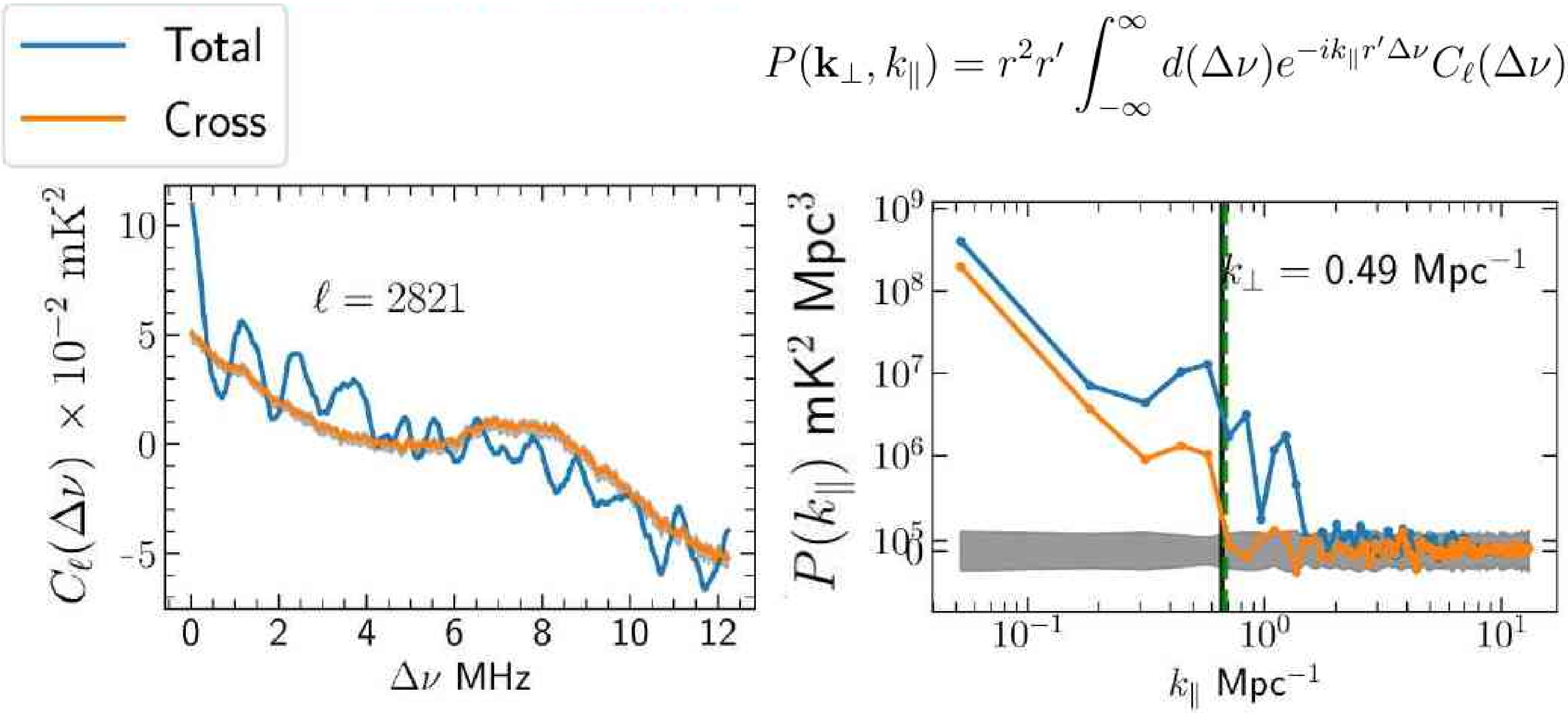

Cylindrical PS and X

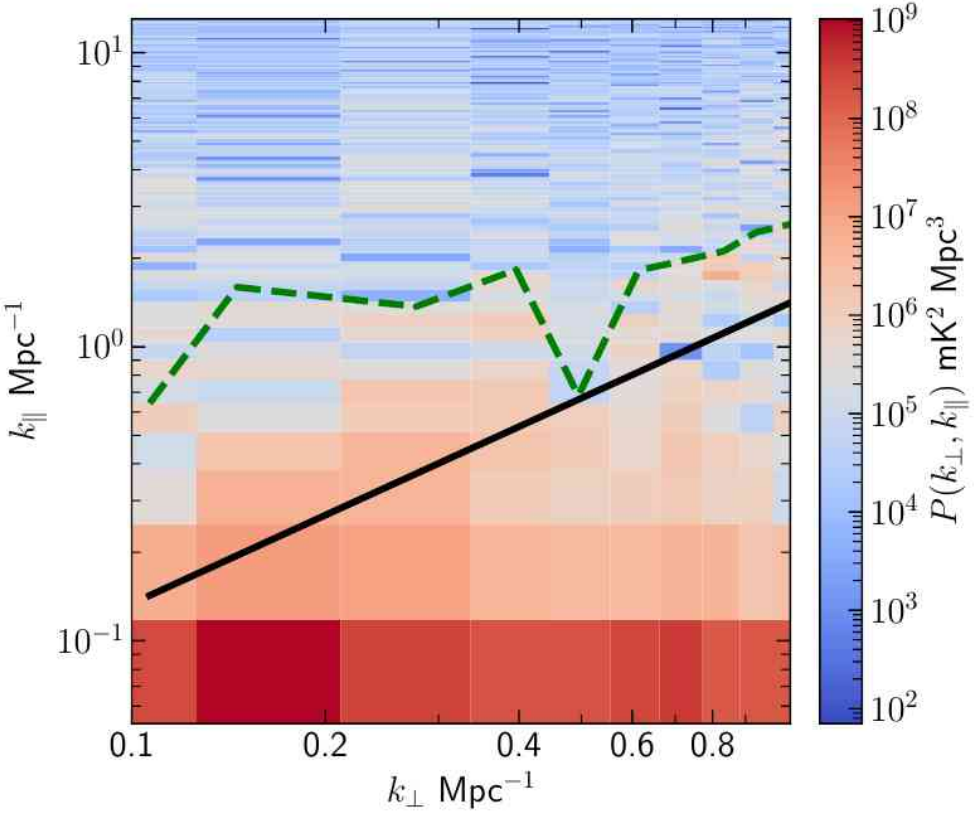

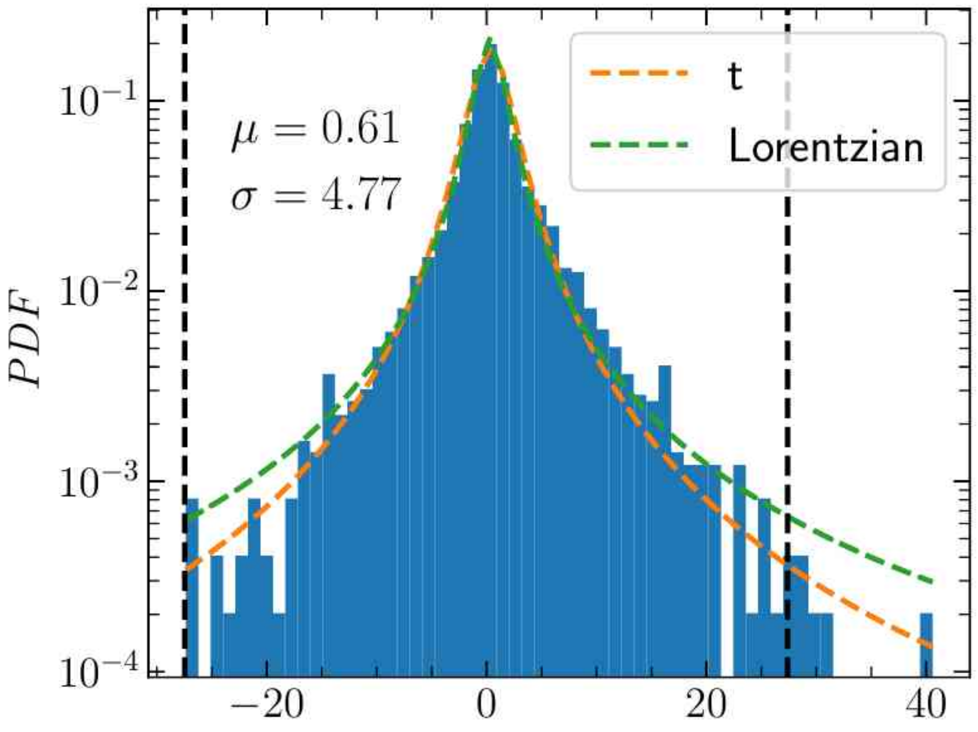

$$X = \frac{P(k_\perp, k_\parallel)}{\delta P_N(k_\perp, k_\parallel)}.$$

Foreground Avoidance

MLE for Spherical PS

$$C_{\ell_a}(\Delta\nu_n) = \left[C_{\ell_a}(\Delta\nu_n)\right]_{FG} + \left[C_{\ell_a}(\Delta\nu_n)\right]_{T} + \left[C_{\ell_a}(\Delta\nu_n)\right]_{R}$$

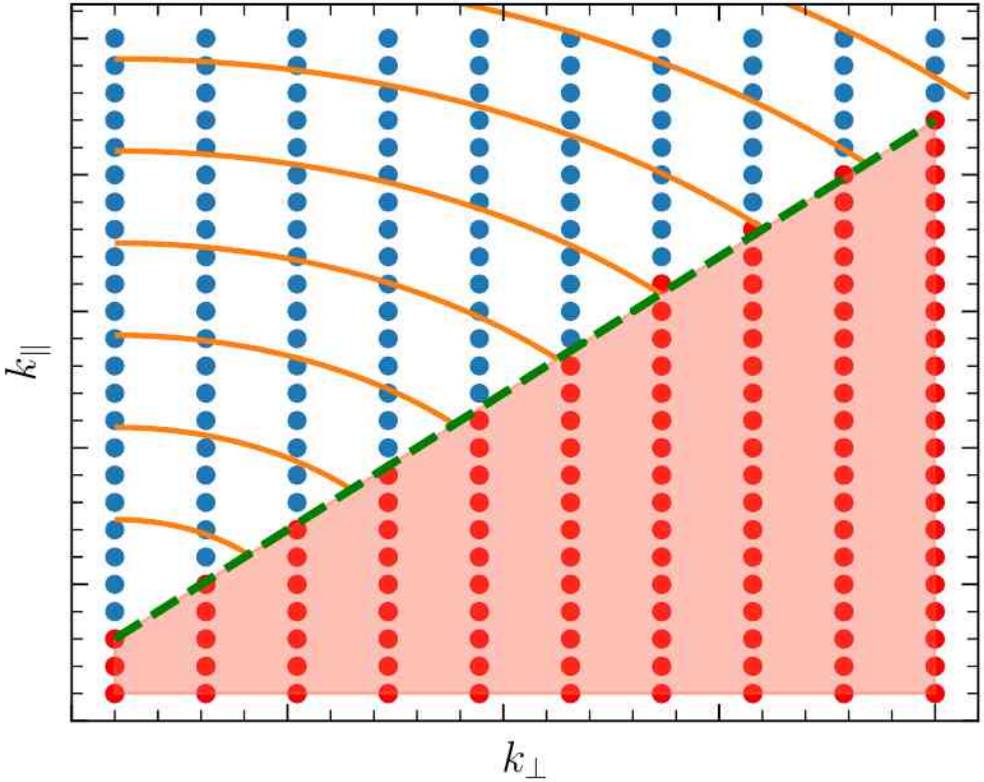

$$\chi^2 = \sum_{a,n,m} \left[C_{\ell_a}(\Delta\nu_n)\right]_R \mathbf{N}^{-1}_{nm} \left[C_{\ell_a}(\Delta\nu_m)\right]_R$$

Mean-squared brightness

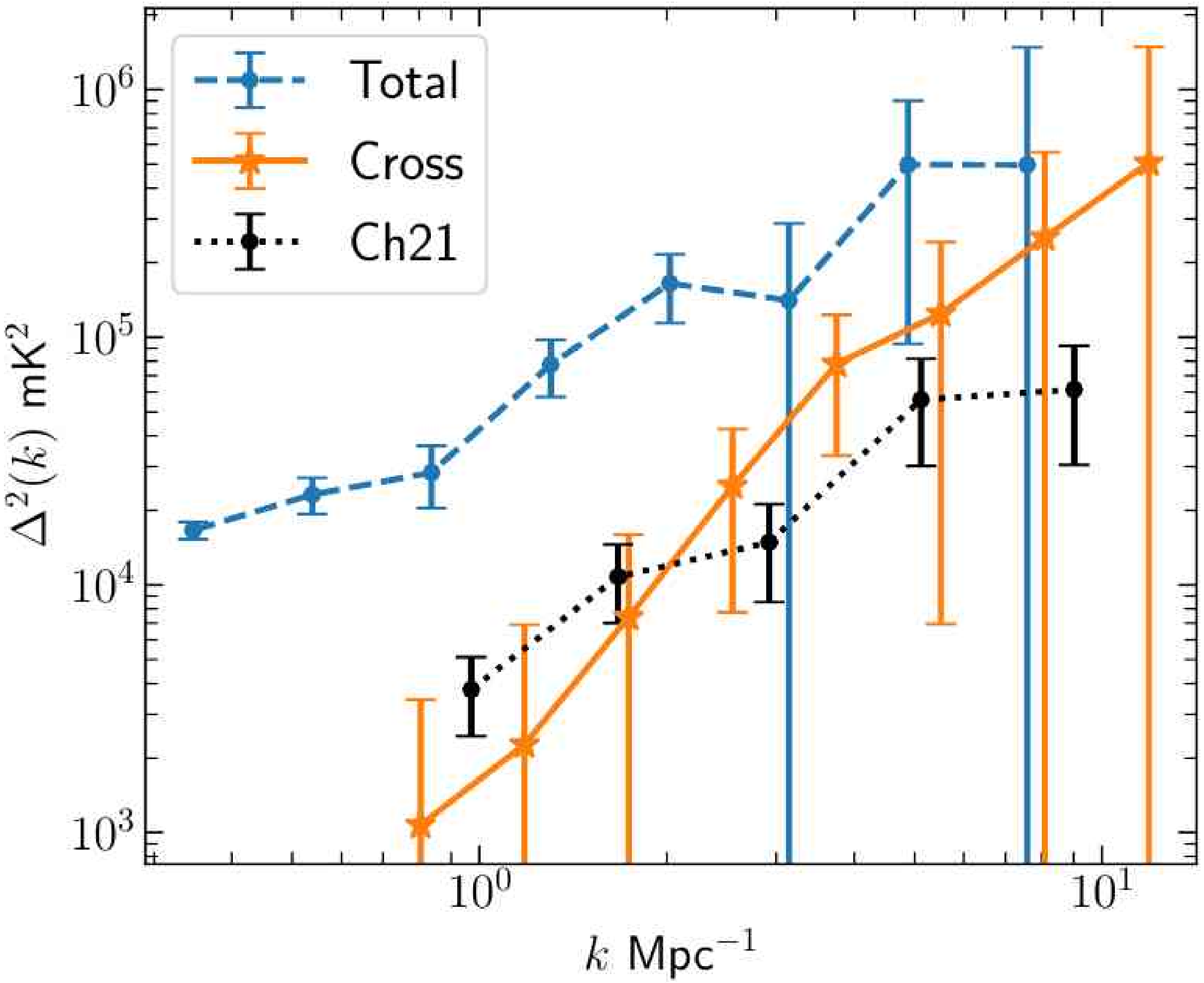

$$\Delta^2(k) \equiv k^3 P(k)/2\pi^2$$

Upper limits

k Mpc^{-1}	$\Delta^2(k)$ $(\mathrm{mK})^2$	1σ $(\mathrm{mK})^2$	SNR	$\Delta^2_{UL}(k)$ $(\mathrm{mK})^2$	$[\Omega_{\mathrm{HI}} b_{\mathrm{HI}}]_{UL}$
0.804	$(32.75)^2$	$(34.42)^2$	0.905	$(58.67)^2$	0.072
1.181	$(47.64)^2$	$(48.19)^2$	0.977	$(83.15)^2$	0.089
1.736	$(86.05)^2$	$(65.31)^2$	1.736	$(126.24)^2$	0.121
2.551	$(158.47)^2$	$(93.18)^2$	2.892	$(206.11)^2$	0.177
3.748	$(279.47)^2$	$(149.74)^2$	3.483	$(350.64)^2$	0.273
5.507	$(352.76)^2$	$(242.38)^2$	2.118	$(491.87)^2$	0.350
8.093	$(502.73)^2$	$(391.31)^2$	1.651	$(747.65)^2$	0.490
11.892	$(712.14)^2$	$(698.77)^2$	1.039	$(1218.07)^2$	0.589

$$P_T(\mathbf{k}) = [\Omega_{\mathrm{HI}} b_{\mathrm{HI}}]^2 \bar{T}^2 P^s_m(\mathbf{k})$$

$$\bar{T}(z) = 133\,\mathrm{mK}\,(1+z)^2 \left(\frac{h}{0.7}\right)\left(\frac{H_0}{H(z)}\right)$$

Pal et al. 22

k Mpc^{-1}	$\Delta^2(k)$ $(\mathrm{mK})^2$	1σ $(\mathrm{mK})^2$	$\Delta^2_{UL}(k)$ $(\mathrm{mK})^2$	$[\Omega_{\mathrm{HI}} b_{\mathrm{HI}}]_{UL}$
0.347	$(128.91)^2$	$(25.79)^2$	$(133.97)^2$	0.230

Chakroborty et al. 21

k Mpc^{-1}	z = 2.19 Δ^2_I mK^2	$\Delta^2_{I,\,err}$ mK^2
0.97	$(61.49)^2$	$(36.50)^2$

$[\Omega_{\mathrm{HI}} b_{\mathrm{HI}}] \lesssim 0.11$

Summary & Future Goals

1. 21-cm signal holds a lot of potential
2. Foregrounds are the primary challenge
3. TGE – a PS estimator: **deals with foregrounds and other challenges**
4. Cross-correlation is promising
5. Foreground removal (in preparation)

Thank You !

Additional Slides

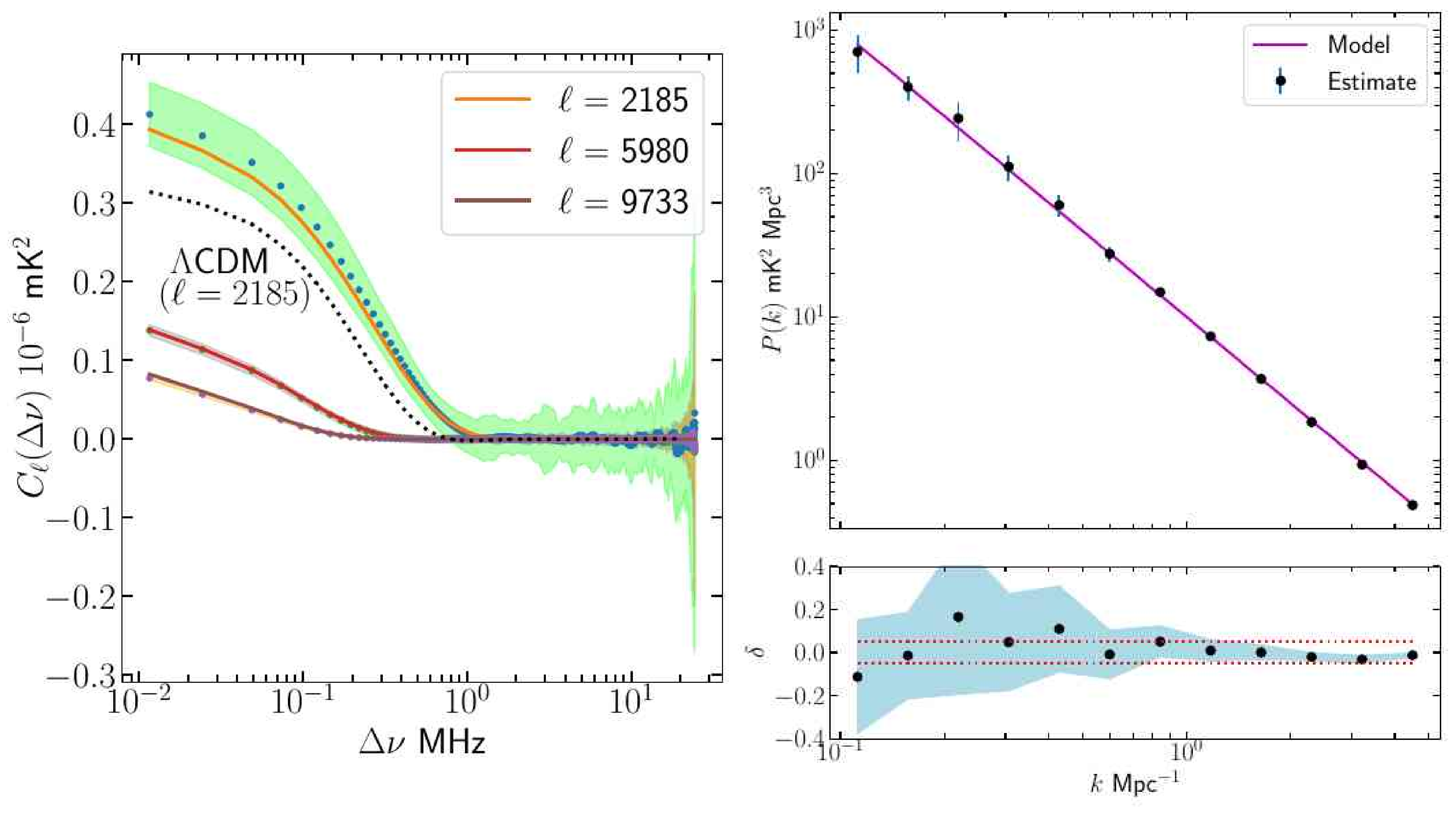

$\ell = 2185$
$\ell = 5980$
$\ell = 9733$
ΛCDM
$(\ell = 2185)$
$C_\ell(\Delta\nu)\ 10^{-6}$ mK^2
$\Delta\nu$ MHz
Model
Estimate
$P(k)$ mK^2 Mpc^3
δ
k Mpc^{-1}

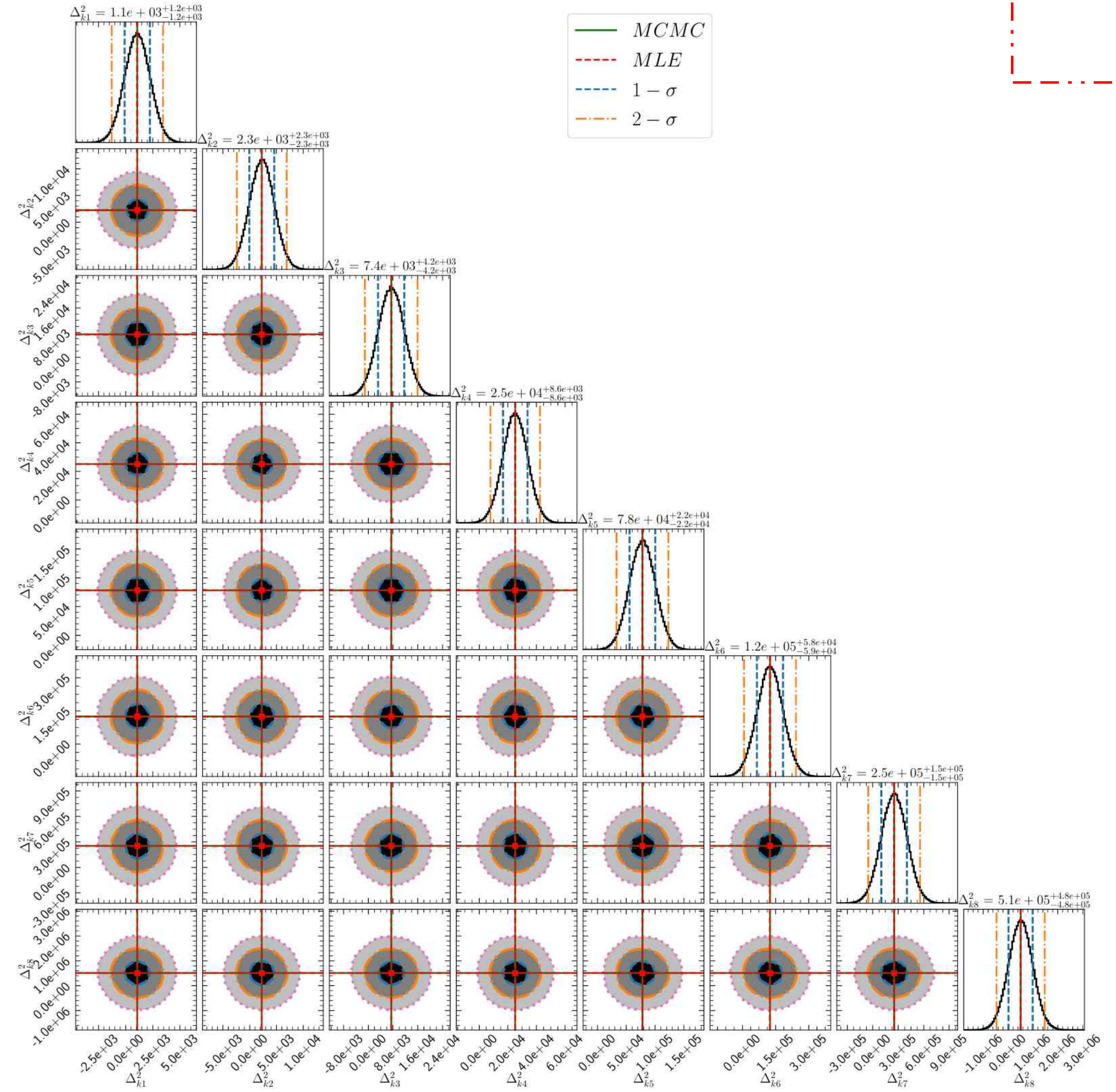

MCMC Analysis

k Mpc^{-1}	$\Delta^2(k)$ $(\mathrm{mK})^2$	1σ $(\mathrm{mK})^2$	SNR	$\Delta^2_{UL}(k)$ $(\mathrm{mK})^2$	$[\Omega_{\mathrm{HI}} b_{\mathrm{HI}}]_{UL}$
0.804	$(32.71)^2$	$(34.33)^2$	0.908	$(58.55)^2$	0.072
1.181	$(47.60)^2$	$(48.17)^2$	0.976	$(83.11)^2$	0.089
1.736	$(86.16)^2$	$(65.19)^2$	1.747	$(126.19)^2$	0.121
2.551	$(158.63)^2$	$(93.12)^2$	2.902	$(206.17)^2$	0.177
3.748	$(279.53)^2$	$(149.72)^2$	3.486	$(350.67)^2$	0.273
5.507	$(353.38)^2$	$(242.35)^2$	2.126	$(492.29)^2$	0.350
8.093	$(501.87)^2$	$(390.10)^2$	1.655	$(745.81)^2$	0.488
11.892	$(711.87)^2$	$(696.66)^2$	1.044	$(1215.50)^2$	0.588